

Simulation of Precipitation Reactions in Reverse Micelles

Rajdip Bandyopadhyaya, R. Kumar,[†] and K. S. Gandhi*

Department of Chemical Engineering, Indian Institute of Science, Bangalore 560 012, India

Received January 26, 2000. In Final Form: June 5, 2000

Precipitation involving mixing of two sets of reverse micellar solutions—containing a reactant and precipitant respectively—has been analyzed. Particle formation in such systems has been simulated by a Monte Carlo (MC) scheme (Li, Y.; Park, C. W. *Langmuir* **1999**, *15*, 952), which however is very restrictive in its approach. We have simulated particle formation by developing a general Monte Carlo scheme, using the interval of quiescence technique (IQ). It uses Poisson distribution with realistic, low micellar occupancies of reactants, Brownian collision of micelles with coalescence efficiency, fission of dimers with binomial redispersion of solutes, finite nucleation rate of particles with critical number of molecules, and instantaneous particle growth. With the incorporation of these features, the previous work becomes a special case of our simulation. The present scheme was then used to predict experimental data on two systems. The first is the experimental results of Lianos and Thomas (*Chem. Phys. Lett.* **1986**, *125*, 299, *J. Colloid Interface Sci.* **1987**, *117*, 505) on formation of CdS nanoparticles. They reported the number of molecules in a particle as a function of micellar size and reactant concentrations, which have been predicted very well. The second is on the formation of Fe(OH)₃ nanoparticles, reported by Li and Park. Our simulation in this case provides a better prediction of the experimental particle size range than the prediction of the authors. The present simulation scheme is general and can be applied to explain nanoparticle formation in other systems.

1. Introduction

One of the methods of producing particles of nano-dimensions involves the use of swollen reverse micelles. The aqueous pools (containing a dissolved reactant) in these systems are of nanodimensions and act as micro-reactors for conducting precipitating reactions. The second reactant (precipitant) can be a gas, a solute soluble in the continuous phase, or another set of swollen reverse micelles. Each of these methods has been employed by various investigators to produce nanoparticles. For example, nanoparticles of CaCO₃ are industrially produced in situ during the process of overbasing. The swollen reverse micellar solution in this case is stirred with micrometer-size Ca(OH)₂ particles and the suspension contacted with CO₂ passed as gas.¹ Instead of passing a gaseous reactant, nanoparticles of Ni₂B have been formed of Ni(NO₃)₂ and NaBH₄, when the latter (a precipitant soluble in the oil phase) is added to the micellar solution containing Ni(NO₃)₂.² In both the above methods the molecules of the precipitant reach the cores of the reverse micelles through mass transfer. There is an alternate way of bringing the reactant and precipitant together, in which each reactant is taken as a micellar solution and the two solutions mixed together. Here the two reactants reach each other through collisions and coalescence of micelles. A number of investigations based on the last method have been reported in the literature, which not only show that nanoparticles can be formed through liquid–liquid precipitation, but also report the influence of important parameters, such as size of the aqueous cores, the concentration of the two reactants, and excess of precipitant used, on the particle size distribution (PSD).

Apart from the experimental investigations, an effort at quantitative description has also appeared in the literature.

When two micellar solutions each containing a reactant are mixed, the reaction proceeds through collisions and coalescence. One of the reactants may be in excess of the stoichiometric requirements. To assess the extent of the reaction, one therefore needs to follow the distribution of both the reactant species in the micelles. In addition, the liquid phase product distribution, as well as the product particle size distribution, also need to be followed. An analysis of this system would normally result in multivariate population balance equations (PBEs) for both the “particle containing” and “particle free micelles”, in terms of the reactants and products as state variables. The solution of these resulting PBEs would be quite involved.

Instead, the same analysis can be accomplished relatively easily through Monte Carlo (MC) simulation of the precipitation process. Our objective in this paper is to develop a general Monte Carlo (MC) simulation scheme for predicting size and size distribution of particles obtained by precipitation in reverse micelles.

2. Previous Simulation

Li and Park³ have recently published a simulation method for such a reaction scheme. They have presented a simple scheme to calculate particle size distribution (PSD) at various stages of a precipitation process, conducted by mixing two reverse micellar solutions. They considered the following steps.

Two micelles chosen randomly from the whole population are allowed to collide, fuse, and redisperse. Upon collision and fusion, the contents of the two are completely mixed. When the two micelles happen to be one from each population, containing the two reactants A and B, respectively, the product C(l) is formed by instantaneous reaction. Furthermore, the liquid product C(l) is assumed to nucleate instantaneously into a solid particle, called P(s). Micelles containing such solid particles are henceforth termed nucleated micelles, whereas the others are known as nonnucleated micelles. Thus the following sequence of steps is considered.

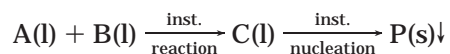
* To whom correspondence should be addressed.

[†] Also at Jawaharlal Nehru Centre for Advanced Scientific Research, Bangalore, India.

(1) Roman, J.; Hoornaert, P.; Faure, D.; Biver, C.; Jacquet, F.; Martin, J. *J. Colloid Interface Sci.* **1991**, *144*, 324.

(2) Nagy, J. B. *Colloids Surf.* **1989**, *35*, 201.

(3) Li, Y.; Park, C. W. *Langmuir* **1999**, *15*, 952.



On redispersion, the particle P(s) goes into any one of the daughter micelles. The remaining unreacted amount of the reactant which was present in excess is equally distributed between the two micelles. When a nucleated micelle collides with a nonnucleated one, then any further product C(l), if formed, by reaction between these two micelles, was assumed to instantly result in growth of the existing solid particle. There is no further nucleation or any redistribution of C(l) at this stage. Excess A or B molecules are as usual equally redistributed. Finally, when the two colliding micelles each have a particle, the additional product C(l) formed grows onto the existing particles in ratio of their surface areas.

When the two colliding micelles (whether nucleated or not) put together have only one of the reactants, then the total amount of this reactant is equally redistributed. Furthermore, the particles of two nucleated micelles never exchange during collisions, and collisions involving three micelles are not allowed.

Due to instantaneous reaction, no micelle at any instant can have both A and B simultaneously. On the other hand, due to instantaneous nucleation, no micelle can contain C(l) for a finite time. Finally, instantaneous growth ensures that each nucleated micelle can contain only one particle.

The authors take a total of N ($>60\,000$) micelles and designate the state of each micelle by a vector of three variables (C_a , C_b , V_p). These indicate the concentrations of the reactants A and B and the volume of the solid particle P(s), respectively. The concentrations are scaled with the respective initial concentrations of A and B in a micelle, while volume is scaled with the volume of a reference particle. The latter is taken as the one formed upon mixing two initial micelles containing A and B at their respective starting concentrations. To start with, the micelles are monodispersed both in size and concentration. Half of them contain only A, while the other half contain only B, having nondimensional state vectors (1 0 0) and (0 1 0), respectively. As collision and fusion proceed, slowly A and B get dispersed over all the micelles. This is kept track of by updating the state vectors. Nucleation of a particle results in a nonzero entry in the third position of the nucleated micelle's state vector, shown above.

They quote the experimental system of Pillai,⁴ wherein two water in octane microemulsions, containing aqueous solutions of $\text{Fe}(\text{NO}_3)_3$ and NH_3 , respectively, were taken. The continuous phase had cetyltrimethylammonium bromide (CTAB) and 1-butanol as surfactant and cosurfactant, respectively. The measured average micellar size was 30 nm, and the concentration of $\text{Fe}(\text{NO}_3)_3$ in the micelles was 0.05 M. Thus the particle size corresponding to the initial amount of reactant in a micelle was 3.5 nm and was used as the scaling size for reporting particle size distribution. In their simulation, Li and Park³ observe spikes in the PSD in the early stages of precipitation, at low to moderate conversions. Subsequently, at high conversions, simulation shows the appearance of very fine particles by reaction between residual amounts of reactants. This broadens the PSD considerably and produces a bimodal distribution, in the form of a small hump below the mode of the distribution. In contrast to the experimental particle size range of 3–7 nm reported by Pillai,⁴ simulation of Li and Park³ at 98% conversion showed the

range to be 0.2–4.7 nm, with a mode at 3.85 nm. Furthermore, bimodality predicted by the model was not observed in the experiments.

The authors rightly argue that broadening of the PSD is due to increasing number of ineffective collisions at high conversions, which simply redistribute the unreacted amount in the daughter micelles and encourage nucleation of fine particles. Thus they demonstrate through their simulation that the PSD indeed becomes narrower if one of the reactants is quickly depleted before the number of ineffective collisions become dominant. This they achieve by taking one reactant in excess (in a ratio of 4:1), in the beginning of the simulation. Not only are the fines eliminated as a result but the mode also shifts to the scaling size and becomes more prominent.

However there are a number of assumptions of this simulation which make it rather restrictive. First, the authors have considered continuous concentration variables (C_a , C_b) to monitor the state of the micelles. This is valid only when the number of molecules dissolved in a micelle is quite high which generally is not the case. Many a time (for example, in carbonation of lime or formation of CdS), one is interested in systems where very few molecules of solute are present per micelle and the former criterion is not satisfied. Thus it becomes necessary to account for the discrete number of molecules. Further, at low occupancy, the solute is known to be Poisson distributed in micelles and the equal exchange of solute in the redispersion process used by Li and Park would not be consistent.

In the literature, attention has been paid to the general problem of solubilize exchange and redistribution during fusion–fission of micelles. In particular, two papers by Hatton et al.⁵ and Barzykin et al.⁶ have addressed the issue of reaction kinetics in small systems, by analyzing the influence of different exchange and redistribution mechanisms on the course of a reaction. However, their focus has been on reactions elucidating the structure and exchange rates in reverse micelles, such as stopped and continuous flow fluorescence experiments, luminescence quenching, etc. These papers thus do not deal with nanoparticle formation.

Second, not only reaction and particle growth, but also nucleation has been treated as instantaneous, irrespective of whether the minimum molecules required for forming a nucleus are present or not. As a result, for any precipitating system, their simulation would always predict the same form of PSD and with the same nondimensional values, without any system specific feature. Furthermore, all collisions are assumed to result in coalescence, and redispersion of excess solute is also done in equal amounts. There is, hence, neither any rate law nor any solute distribution and exchange rule, which could be taken as dependent on the chemical constituents of the experimental system.

The present work describes a more general and less restrictive framework for simulation of reactions between two sets of swollen reverse micelles, with each containing a separate reactant.

3. New Simulation Procedure

The algorithm of our simulation is presented in Figure 1. Details of the function “binomial” and calculations of PSD (appearing in Figure 1) are discussed in Appendices A and B, respectively. In the subroutine “Move” in Figure

(4) Pillai, V. K. Quoted in Li and Park, 1999. Ph.D. Thesis, University of Florida, Gainesville, FL, 1995.

(5) Hatton, T. A.; Bommarius, A. S.; Holzwarth, J. F. *Langmuir* **1993**, *9*, 1241.

(6) Barzykin, A. V.; Tachiya, M. *J. Phys. Chem.* **1994**, *98*, 2677.

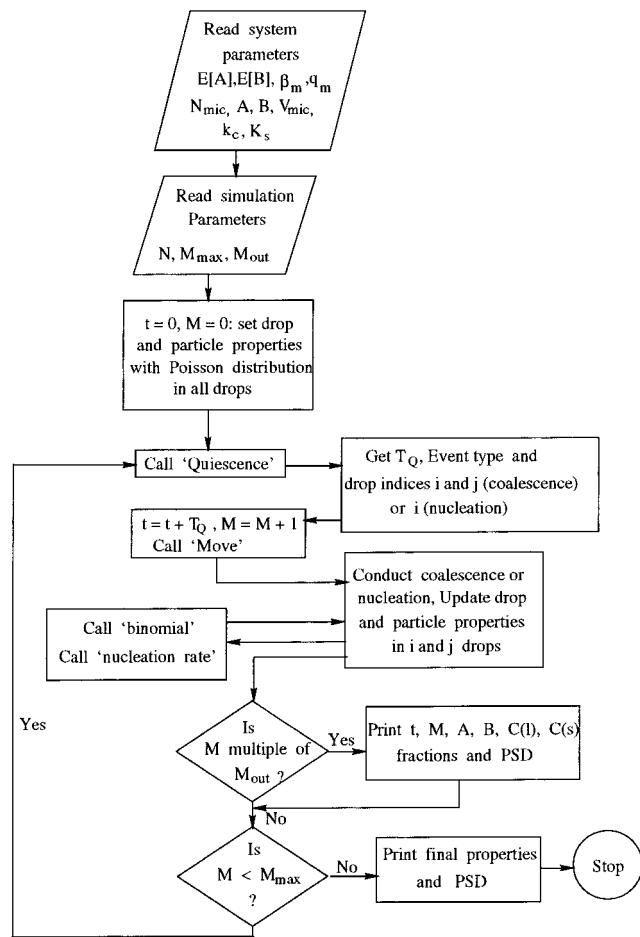
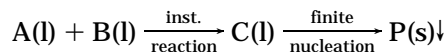


Figure 1. Flowchart of the present MC simulation scheme.

1, we conduct reaction, redistribution of excess reactant and product molecules in the daughter micelles, and nucleation and growth of solid particles. The number of reverse micelles, N , taken for simulation is such that further increase in it has no effect on the final results. A total of 100 000 micelles were taken in the simulation and their states followed in time. This was found to be adequate for getting converged results. Half of them initially contained a solution of reactant A, and the other half contained the reactant B in solution. The numbers of molecules of both A and B in a micelle are assumed to be distributed in their respective micelle population as per Poisson distribution, the mean of the distributions being the respective mean number of molecules of A and B in the micelles. When two micelles containing A and B, respectively, coalesce, product in dissolved form, $C(l)$, is instantaneously formed, so that the limiting reactant is completely consumed. The coalesced dimer breaks immediately, conserving the total number and size of micelles. On redispersion, the excess reactant (A or B) and the dissolved liquid product ($C(l)$) are distributed between the two daughter micelles, in accordance with binomial redistribution. Binomial redistribution has been used as it is consistent with the observed Poisson distribution for dissolved species.

Nucleation however is not instantaneous, unlike the previous simulation. As the process advances, some of the micelles nucleate following a specific rate depending on supersaturation as well as the presence of a minimum number of molecules required for formation of a stable nucleus. The steps involved here can be depicted as follows:



When these nucleated micelles have access to liquid-phase product (through coalescence with a nonnucleated micelle), the particle inside the former grows instantaneously. Product required for growth is either formed through possible reaction during the coalescence of this micelle with a second, or is already available in the second coalescing micelle. The state of all the particles as well as reactant and liquid-phase product is kept track of as a function of time. The processes of coalescence, reaction, redistribution, nucleation, and growth continue until a time invariant state is reached.

When either nucleation or coalescence occur, the state of the system is changed. To evaluate the dynamics of the process, it is necessary to keep track of each event as a function of time. For example, it is necessary to decide whether the next event would be coalescence or nucleation and what would be the interval between two events. Kinetics of the overall process would depend on the number of these time intervals. In the present simulation, we have used the method of interval of quiescence⁷ to decide on the nature and the time interval between subsequent events. This method simulates a process of randomly occurring events while ensuring that the mean rate of the process is conserved. It proposes that in processes where events occur independently, such as the one being considered in the present work, (i) the time interval between events follows a Poisson distribution, (ii) the meantime interval between two successive events is equal to the inverse of the sum of mean frequencies of all the events possible, and (iii) the probability of occurrence of an event is proportional to the average frequency of that event.

The basic procedure is as follows. First the total frequency of all events including all the N micelles in the simulation is calculated:

$$f_t = f_c + f_n \quad (1)$$

Here f_t is the time variant total frequency whereas f_c and f_n are coalescence–redispersion and nucleation frequencies, respectively. The latter is a function of time, since nucleation rate of each micelle varies during the simulation. Therefore after every event, f_t is evaluated and the coalescence–redispersion and nucleation events are distributed in the ratio of f_c/f_t and f_n/f_t , respectively. To decide what event is to occur next, a sample value is drawn from a uniform random number generator, $U[0,1)$, lying between 0 and 1. If the value falls between 0 and f_c/f_t , the event is coalescence–redispersion; otherwise it is nucleation. To evaluate the quiescence time, we use the fact that the quiescence time interval T_Q is a continuous random variable and follows an exponential distribution with mean $1/f_t$. This is given later. First the expressions for f_c and f_n are given below,

$$f_c = 1/2 \beta_m q_m N_{mic} N \quad (2)$$

where q_m is the collision rate due to Brownian motion and is given by

$$q_m = \frac{8k_B T}{3\eta} \quad (3)$$

(7) Shah, B. H.; Ramkrishna, D.; Borwanker, J. D. *AIChE J.* **1977**, *23*, 897.

β_m is the coalescence efficiency, which for most situations is less than unity. It is constant for a given simulation run but may change from system to system. Further,

$$f_n = \sum_{i=1}^N k_{n_i}(l) \quad (4)$$

where $k_{n_i}(l)$ is the nucleation rate of the i th micelle, which in general can have $l(\geq 0)$ product molecules. Only micelles having $l \geq k_c$ (the critical number of molecules) contribute to the above summation. For other micelles the nucleation rate is taken as zero.

We use the expression for nucleation rate quoted by Adamson.⁸ The expression for nucleation rate in the i th micelle is the following:

$$k_{n_i}(l) = \begin{cases} 0 & l < k_c \\ IA \exp\left[-\frac{16\pi\sigma^3 V_m^2}{3(k_B T)^3 (\ln \lambda_l)^2}\right] & l \geq k_c \end{cases} \quad (5)$$

where

$$\lambda_l = \frac{[C(l)]_l}{S} \quad (6)$$

is the supersaturation in the liquid phase, with concentration of liquid product molecules given by

$$[C(l)]_l = \frac{l}{N_A V_{\text{mic}}} \quad (7)$$

The first term in eq 5 is a mathematical statement that nucleation rate is zero if the number of solute molecules present in a micelle are less than the critical value.

So, each of the processes of reaction, nucleation, growth, and coalescence-redispersion may change $[C(l)]_l$ and hence nucleation rate of a given micelle, making f_n a function of time.

Substituting the expressions for f_c and f_n in eq 1, we obtain

$$f_t = 1/2\beta_m q_m N_{\text{mic}} N + \sum_{i=1}^N k_{n_i}(l) \quad (8)$$

We then get the random, quiescence time interval values from the equation

$$T_Q = -\frac{\ln(1 - u_1)}{f_t} \quad (9)$$

where u_1 is a sample value obtained from the uniform random number generator $U(0,1)$.

Once a nucleation event is due, any of the supersaturated micelles having critical number or more of $C(l)$ molecules can nucleate. The probability that a particular micelle would nucleate is proportional to its nucleation rate and is hence decided by generating a random number. Collision rate and coalescence efficiency, on the other hand, are independent of the state of the micelle. So all collision pairs have equal probability of coalescing, once a coalescence-redispersion event is due.

The system is updated after each coalescence-redispersion or nucleation, till the simulation clock reaches

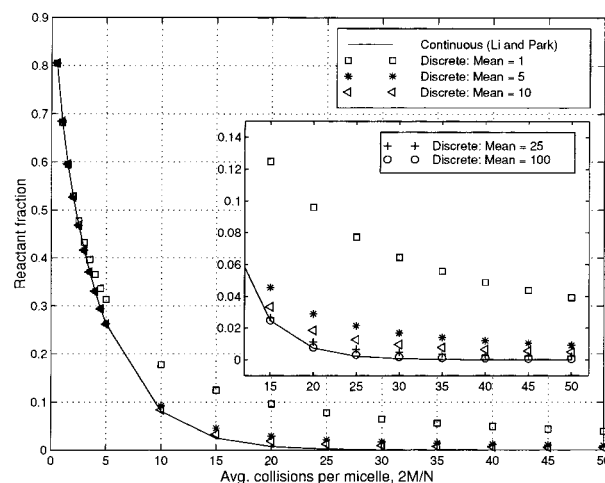


Figure 2. Effect of discrete number of molecules (equal occupancy = 1, 5, 10, 25, 100) on conversion of reactant with time, in Li and Park's simulation. The inset shows effects at high conversions.

the desired conversion to solid particles. The system size in terms of number of micelles, N , is increased, till conversion and PSD show no deterministic change.

4. Comparison of Simulation Results

To explore the implications of various assumptions made in the present work, it was decided to first relax the appropriate assumptions to correspond to the previous model³ and then incorporate the assumptions one by one and investigate their effects on the predictions. To conform to their assumptions, we eliminate initial Poisson distribution of reactants, binomial redispersion of excess solute, critical nucleus and nucleation rate laws from our quiescence interval simulation. The notion of quiescence interval automatically gets eliminated as the rate for nucleation is removed. The coalescence efficiency is treated as unity, and their rules of particle growth are adopted. This results in a simplified code analogous to theirs. They have used 50 000 micelles or more of each reactant to ensure convergence. In the present work also, on using 50 000 micelles of each reactant and under the above conditions, the predictions made by Li and Park³ could be correctly reproduced (comparison not shown) from our simulation.

4.1. Implications of Using a Discrete Number of Molecules Instead of Continuous Concentration in a Micelle. The average number of reactant molecules in a micelle can vary from less than one to many hundreds. A comparison was made between the use of a discrete number of molecules in a micelle and continuous concentration to decide whether it is at all necessary to deal in terms of discrete population of molecules. For this purpose, simulation was conducted by treating both the reactant and product amounts in a micelle in terms of a discrete number of molecules, starting from 1 to 10 000 molecules per micelle. Whenever redistribution (when two nucleated micelles coalesce and redispersion) was necessary, the molecules were distributed equally to the two micelles. In the case of an odd number of molecules, one micelle is given a higher integer and the other one lower. All other aspects were same as those of the authors.

The results of fractional reactant variation as a function of the average number of collisions undergone by a micelle are shown in Figure 2. The abscissa is reflective of the time of the process. The symbols are results from the discrete version, with different occupancies, shown in the

(8) Adamson, A. W. *Physical Chemistry of Surface*, 5th ed.; John Wiley & Sons: New York, 1990; p 369.

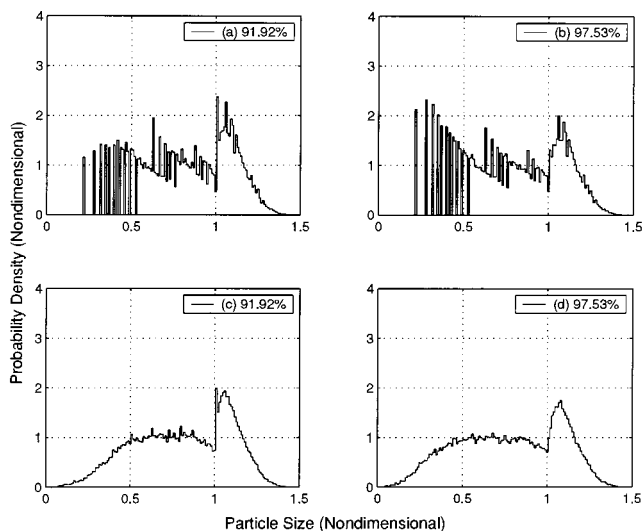


Figure 3. Effect of discrete number of molecules (equal occupancy = 100, in a and b) on PSD of Li and Park's simulation with continuous concentration (c and d) at various conversions: (a) 91.92%, (b) 97.53%, (c) 91.92%, (d) 97.53%.

legend, whereas the solid line corresponds to those obtained from use of continuous concentration. As the number of molecules in a micelle is increased from 1 to 10, a progressive convergence in the fraction of unconverted reactant toward the solid line is observed. Compared to the continuous case, conversion is quite slow for an occupancy of 1 molecule/micelle, especially toward the end. With increase to 5 and then to 10 molecules/micelle, the results converge to the continuous case for up to about 90% conversion. However, for conversion of 90% and beyond, the convergence is not satisfactory even with 10 molecules. The results at higher conversions are shown on enlarged scale as inset in Figure 2. It is seen that with 100 molecules/micelle, it is possible to reproduce the overall conversion predicted in the continuous mode. Thus it seems that with 100 molecules/micelle, the concept of continuous concentration can be applied, as far as the conversion plot is concerned, whereas at lower occupancy there is need to consider the actual number of molecules per micelle.

However there is substantial difference in PSDs even at 100 molecules, from the PSDs obtained with continuous concentration, as seen in Figure 3. In this figure, the upper row plots correspond to simulation with 100 molecules, whereas the corresponding plots with continuous concentration variable are given in the bottom row. The differences at these conversions are large and obvious. At occupancies of unity or 5 or 10, the differences are still larger (not shown here). It is only when the occupancies reach 10 000 molecules that the two methods yield the same result. Most precipitation reactions involve less than 100 molecules/micelle. Hence it is more appropriate to use a discrete number of molecules in a micelle rather than employing the notion of a concentration while performing the simulation.

4.2. Effect of Redistribution Mode on Conversion and PSD. Another important change made in the present work is that the liquid contents of the dimer are distributed in an unequal fashion between the two daughter micelles, instead of being distributed equally. To study the sole effect of the mode of redistribution, we have incorporated only this feature in the simulation scheme of Li and Park, using continuous concentration variables analogous to theirs. The results obtained by us from these simulation runs for random redistribution are shown in Figures 4 and

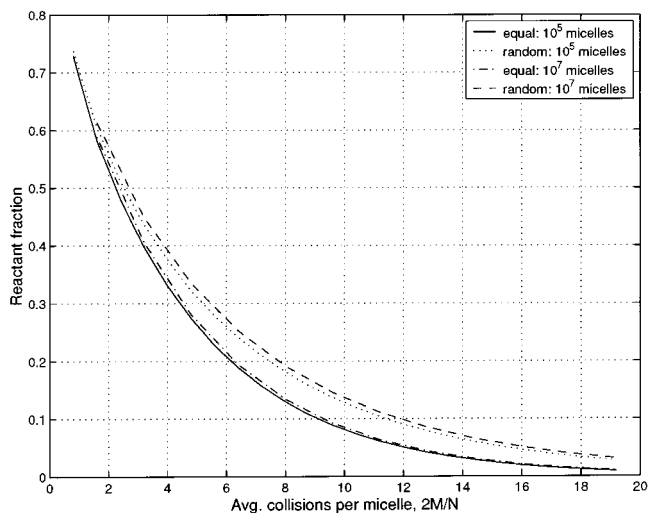


Figure 4. Effect of random redistribution of solutes and number of micelles taken in simulation on conversion of reactant with time, in Li and Park's simulation.

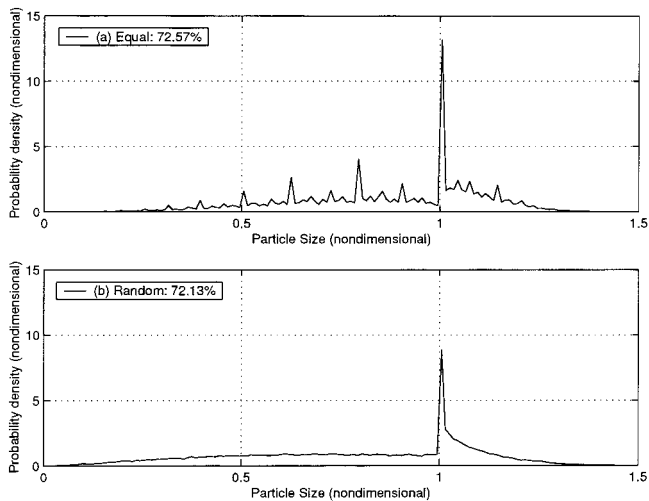


Figure 5. Effect of random solute redistribution on PSD of Li and Park's simulation: (a) equal redistribution, 72.57%, (b) random redistribution, 72.13%.

5. The fraction of solute going to one of the daughter micelles under random redistribution mode is a uniform random number between 0 and 1. The rest of the solute in the dimer obviously goes to the other daughter micelle.

In Figure 4, the fraction of reactant left is plotted versus the average number of collisions/micelle $2M/N$, for different number of starting micelles and for different modes of redistribution. First we observe that the results obtained are converged for each redistribution mode, as differences between results of 10^5 and 10^7 micelles are not significant. It is seen that random redistribution significantly reduces conversion, for the same average number of collisions a particular micelle encounters. This is due to the fact that, in random mode, there is a broader distribution in micellar occupancies. This generally results in a large inequality in the amounts of two reactants coming together in a dimer. Since extent of reaction then is restricted only to as much as the amount of limiting reactant in the dimer, it causes less reaction during each fusion.

Figure 5 compares representative PSDs at $\sim 72\%$ conversions. The PSD for random redistribution is seen to be smoother, cutting off the spikes. This indicates that redistribution is unlikely to be equal, since spikes are not seen in any real experiment, at any stage of conversion.

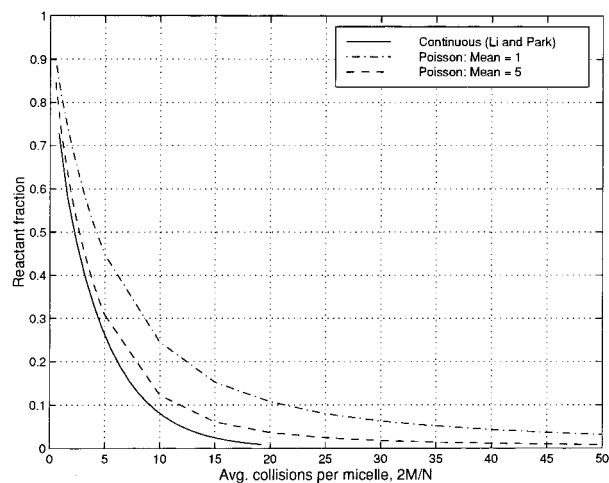


Figure 6. Effect of initial Poisson distribution of reactants (mean occupancy = 1, 5) and subsequent binomial redistribution of solutes on conversion of reactant with time, in Li and Park's simulation.

Some sort of unequal redistribution, not necessarily according to uniform random fraction, is closer to reality. Binomial redistribution, for example, is known to preserve Poisson occupancy of dissolved solutes, and is hence used in our MC simulation as a model for unequal redistribution. It is expected to bear similar influence as shown here for random redistribution.

4.3. Effect of Nonuniform Initial Reactant Occupancy in Micelles. Instead of all micelles having an equal amount of reactant, the assumption in the present model is that initially itself the reactant is distributed following Poisson statistics. This is an assumption which has been shown to be valid by many investigators working in this field. Since Poisson distribution requires an integer number of reactant molecules to be put in different micelles, we naturally work with the simplified, discrete version of our code. Also when we start with a Poisson distribution, it is natural to relocate the excess reactant and product molecules of the dimer into the redispersed pair, according to a binomial distribution. Binomial law also ensures that both the micelles get an integer number of molecules. We find from our computations that such a mechanism preserves the original Poisson distribution of a single reactant in the absence of any reaction. We would however have nonstationary Poisson distributions of the reactant populations, because the overall number of molecules of reactants decreases with time.

Calculations made with the above considerations are shown in Figure 6. It is seen that conversion is lower when Poisson distribution holds since, with many micelles being empty, it results in several infructuous (nonreactive) collisions. The fraction of empty micelles is higher when the Poisson mean is lower; such collisions are more prevalent in case of a mean of one than for a mean of five.

We now discuss the PSDs for assessing the effect of initial Poisson occupancy and binomial redistribution. At mean molecule numbers of 1 and 5, they do not have any drastic effect on the results, except to generate some bigger particles. This is because the Poisson distribution generates initial micellar occupancies both greater and smaller than the mean, unlike the previous calculations with equal occupancies. As a result of higher occupancies, one gets a higher fraction of bigger particles in these cases.

4.4. Influence of Nucleation Kinetics on PSD. Finally the role of critical nucleus and nucleation rate during particle formation from liquid-phase product

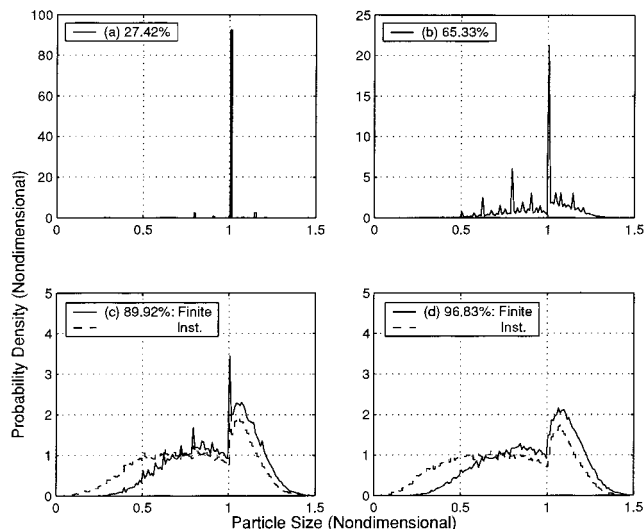


Figure 7. Effect of critical nucleus (critical molecule number = 5) and nucleation rate on PSD of Li and Park's simulation at various solid-phase conversions: (a) 27.42%; (b) 65.33%; (c) 89.92%; (d) 96.83%. Li and Park's results are shown as a dashed line in (c) and (d).

molecules is examined. Figure 7 shows the effect of introducing a critical number of 5 product molecules for nucleation and a finite nucleation rate on the simulation results of Li and Park.³ This plot has been generated from the quiescence interval code, since introduction of nucleation rate requires consideration of collision rates also. A selection of events is therefore necessary to carry out the simulation. However, to focus solely on the aspects of nucleation, other details of the present simulation code have not been included. Thus calculations are made with an initial equal micellar occupancy of 10 000 molecules, which are further redistributed equally too.

Different micelles can therefore have either liquid or solid-phase product, because of finite nucleation rate. Thus we have separate conversion values based on liquid and solid phases, respectively. Until now, we have used conversion based on solid phase, since in an instantaneous nucleation rate simulation, no micelles could have a liquid-phase product. So to maintain uniformity, conversion values shown in Figure 7 (for the cases of finite nucleation) and in later figures are based on conversion to the solid phase. The results of instantaneous nucleation are also presented in Figure 7c,d for comparison of the PSDs obtained in the two cases.

Figure 7a,b shows plots for finite nucleation rate. At these low to moderate conversions, PSDs for finite and instantaneous nucleation rate simulations are the same, and hence, instantaneous case is not shown in these two plots. This is because abundant liquid-phase product is available in the beginning. Thus most of the micelles have a high nucleation rate and contain more than the critical number of molecules. However, toward the end, only some micelles would have liquid product left, and in most cases this would be less than the critical number of molecules. As a result the PSDs from the two simulations would be different. The comparison of these two cases are given in Figure 7c,d. It is seen that incorporation of a critical number of molecules cuts off fine particles from the PSDs for the instantaneous nucleation case (shown as a dashed line). Furthermore, when a finite nucleation rate is imposed, the formation of smaller particles becomes less likely, due to the low supersaturation associated with them. This additional restriction on nucleation of the fines results in increased growth of other particles in the system,

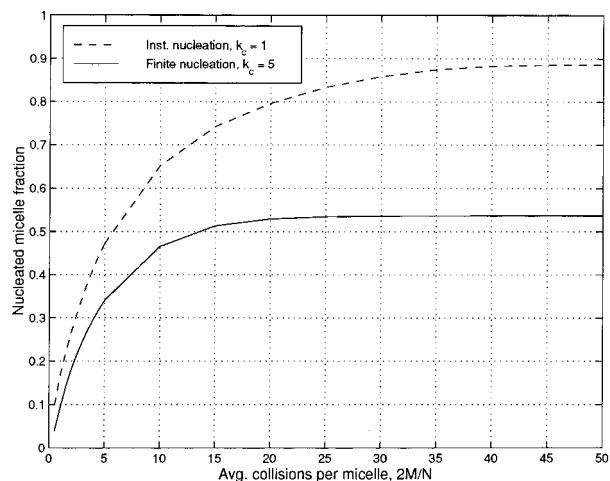


Figure 8. Effect of critical nucleus (critical molecule number = 5) and nucleation rate on temporal variation of the fraction of nucleated micelles formed, in Li and Park's simulation.

extending the maximum particle size to higher values. The number of particles produced, expressed as a fraction of the initial number of micelles—corresponding to the two cases of instantaneous and finite nucleation described above—is shown in Figure 8. Expectedly, the number is less with a finite nucleation rate, with concomitant bigger particles.

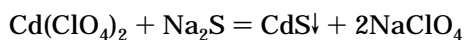
The influence of nucleation parameters (critical nucleus and nucleation rate) will be much more when a smaller number of average molecules are involved. There the use of a Poisson distribution will also be very important, and under some conditions (average number of molecules per micelle being less than the critical number required for nucleus formation), nucleation cannot occur unless a Poisson distribution is incorporated. Thus the influence of various assumptions made in the present code can be large and significant.

5. Prediction of Experimental Results from the Literature

5.1. Experiments on CdS Nanoparticle Formation.

The results of Lianos and Thomas⁹ provide an exhaustive range of variables against which a simulation code can be tested. Thus, the present code is employed to predict their results.

They have prepared CdS nanoparticles by mixing two sets of reverse micelles of AOT in heptane, each containing a different reactant. They took $\text{Cd}(\text{ClO}_4)_2$ and Na_2S respectively in the two sets of micelles. The following reaction takes place among the coalescing micelles:



For all experiments they used constant concentrations of $[\text{AOT}] = 0.5 \text{ M}$ and $[\text{Na}_2\text{S}] = 10^{-4} \text{ M}$, both based on the total dispersion volume. Various excesses of $\text{Cd}(\text{ClO}_4)_2$ were used. Their experimental results are presented in Table 1, from where it is seen that the lowest molecular aggregation number (MAN) obtained by them was 4, indicating that 4 or less molecules of CdS were sufficient to form a nucleus. Other data like micellar concentration, surfactant aggregation number, and water pool radius are also presented in Table 1.

The MAN values reported by them can be converted into particle diameters. Thus using a density of 4.58 g

Table 1. Experimental Results of Lianos and Thomas on CdS Nanoparticle Formation

R	micellar conc (10^{-4} M)	micellar aggregation no.	water pool radius (\AA)	$[\text{Cd}^{2+}]$ (10^{-4} M)	CdS aggregation no. (MAN)
5			21.4	10	5.6 ^a
5	18	278	21	2	4.0
				5	4.7
10				2	12.5
				5	7.2
				10	8.0
32	2.6	1920	76	2	35–45
				5	
				10	11.6

^a $[\text{Na}_2\text{S}] = 5 \times 10^{-4} \text{ M}$.¹¹ The rest are with $[\text{Na}_2\text{S}] = 10^{-4} \text{ M}$.⁹

Table 2. Mean Number of Reactant Molecules/Micelle in CdS Precipitation

R	x	$E[\text{Na}_2\text{S}]$	$E[\text{Cd}(\text{ClO}_4)_2]$
5	2	0.2775	0.555
	5	0.0555	0.2775
	10	0.0555	0.555
32	2	0.3846	0.7692
	10	0.3846	3.846

cm^{-3} for CdS¹⁰ and a molecular weight of 144.47, we find MAN values of 4 and 35 correspond to spherical particle diameters of 7.3 and 15.1 \AA , respectively.

In another paper,¹¹ Lianos and Thomas have prepared CdS, PbS, and CuS nanoparticles in the same fashion. Substitution of $\text{Cd}(\text{ClO}_4)_2$ by CdCl_2 and of Na_2S by $(\text{NH}_4)_2\text{S}$ had little effect on the type or size of CdS particles formed. They reached this conclusion on the basis of the absorption spectra of the CdS particles formed in each case. This is in agreement with the assumption of the present model that reaction kinetics leading to CdS(l) formation is unimportant and reactions can be considered instantaneous in comparison with other processes determining particle size.

For the experiment giving MAN = 5.6 (first entry in Table 1), water pool radius (21.4 \AA) is almost the same as the entry in the next row (21 \AA). Moreover both employ $R = 5$ and $[\text{AOT}] = 0.5 \text{ M}$; hence, we use the same value of micellar concentration of $18 \times 10^{-4} \text{ M}$ for the first experiment tabulated. This is required to calculate mean occupancy in a micelle. However, concentration of limiting reactant Na_2S , as listed in Table 1, was different.

Out of 10 entries in Table 1, only 5 cases were simulated as only those had all the information necessary for simulation. These are summarized in Table 2, where $E[\text{Na}_2\text{S}]$ and $E[\text{Cd}(\text{ClO}_4)_2]$ stand for the initial mean number of molecules of the two reactants in micelles. As emphasized earlier, the mean numbers are very low (less than one) implying the need to consider a discrete number of molecules, distributed in a Poisson fashion.

The values of various parameters used in simulation of CdS nanoparticles are presented in Table 3. Listed are different values of β_m for different experimental conditions. β_m is a reflection of the fraction of collisions that result in fusion. It is influenced by several factors^{12–15} like the nature of the surfactant and cosurfactant, the continuous

(10) Perry, R. H.; Chilton, C. H.; Kirkpatrick, S. D., Eds. *Chemical Engineers' Handbook*, 4th ed.; McGraw-Hill Book Co.: New York, 1963; pp 3–8.

(11) Lianos, P.; Thomas, J. K. *J. Colloid Interface Sci.* **1987**, *117*, 505.

(12) Bommarius, A. S.; Holzwarth, J. F.; Wang, D. I. C.; Hatton, T. A. *J. Phys. Chem.* **1990**, *94*, 7232.

(13) Flethcer, P. D. I.; Howe, A. M.; Robinson, B. *J. Chem. Soc., Faraday Trans. 1* **1987**, *83*, 985.

(9) Lianos, P.; Thomas, J. K. *Chem. Phys. Lett.* **1986**, *125*, 299.

Table 3. Parameters for Simulation of CdS Nanoparticle Formation

variable	value
β_m ($R = 5, x = 2, 5, 10$)	10^{-4}
β_m ($R = 32, x = 10$)	0.01
β_m ($R = 32, x = 2$)	0.10
q_m	$1.097 \times 10^{-11} \text{ cm}^3 \text{ s}^{-1}$
η	0.01 Poise
T	298 K
N_{mic} ($R = 5$)	$1.084 \times 10^{18} \text{ cm}^{-3}$
N_{mic} ($R = 32$)	$1.566 \times 10^{17} \text{ cm}^{-3}$
N	10^5
k_c	2
A	278.42 s^{-1}
V_m	$5.24 \times 10^{-23} \text{ cm}^3$
B	600
K_s	$3.6 \times 10^{-29} \text{ mol}^2 \text{ L}^{-2}$

phase, size of the micelle, and concentration of the dissolved species in the micellar core, etc. It is known that β_m decreases as R is lowered. Therefore, for $R = 5$, low efficiency is used, compared to $R = 32$. Similarly β_m has been pointed out¹⁴ to be a function of concentration. Thus for $R = 32$, different values were used for different x . The values given are in the acceptable range but have been fine-tuned to yield good comparisons. The nucleus has to have less than 4 molecules as particles of that MAN have been experimentally observed. It was found, only on using the lowest possible value of $k_c = 2$, consistently good results for all the cases were obtained. In fact with the extremely low solubility of CdS ($S = \sqrt{K_s}$, see Table 3) and the small micellar water pool radius reported (Table 1), at saturation one can have only of the order of 10^{-12} molecules of CdS(l) in a micelle. Such a low number of molecules implies a huge supersaturation with even 1 or 2 CdS(l) molecules. This justifies the low value of $k_c = 2$, as we know critical number of molecules is inversely proportional to supersaturation.

To get total nucleation frequency in eq 8 at any stage of the simulation, we only look at those micelles having k_c or more CdS(l) molecules and sum up their nucleation rates. The latter is obtained from eq 5. Computations have been made with the value of preexponential factor $A = 278.42 \text{ s}^{-1}$. This same value was used by us earlier.¹⁶ The bracketed term in eq 5, except $\ln \lambda_k$, i.e., the term $16\pi\sigma^3 V_m^2 / 3(k_B T)^3$, is defined as a system specific constant B . Since solid-liquid interfacial tension σ for CdS is not known, we have used a typical value of 100 dyne cm^{-1} , generally valid for other solids; e.g., for CaCO_3 it is 97 dyn cm^{-1} . Using V_m from Table 3, the above-mentioned constant B works out to be 600. To calculate supersaturation λ_k , we use eq 6, with solubility S calculated as $\sqrt{K_s}$.¹⁷ The latter is listed in Table 3. Finally, aqueous core volume, V_{mic} , required in eq 7 was in each case found from water pool radius values of Table 1.

5.2. Simulation of CdS Nanoparticle Formation.

The results of simulation corresponding to experiments tabulated in Table 2 are presented in Table 4, where both experimental and simulation results are given as mean aggregation numbers of CdS molecules. Simulation is able to predict not only the trends but also the quantitative MAN values very closely in most cases. For example, the model correctly predicts the experimental finding that, at

Table 4. Comparison of Experimental and Simulated Prediction of the Molecular Aggregation Number of CdS Nanoparticles

R	x	MAN	
		exptl	simulation
5	2	5.6	5.22
	5	4.0	4.74
	10	4.7	4.83
32	2	35–45	38.85
	10	11.6	13.78

Table 5. Time Scales in CdS Nanoparticle Formation

process	$R = 5$	$R = 32$
	($x = 2, 5, 10$) (s)	($x = 2$ or 10) (s)
coalescence with any micelle (τ_c)	8.41×10^{-4}	$5.82 \times 10^{-6}{}^a$
nucleation in a single micelle (τ_n)	3.45×10^{-3}	$5.82 \times 10^{-5}{}^b$

^a $x = 2$. ^b $x = 10$.

$R = 5$, the MAN values are much lower than at $R = 32$, for the same x .

To explain the results of both experiments and simulation, we compare the relevant time scales, which are given in Table 5. Growth is virtually instantaneous because of small size of micelles. So the number of particles is decided on the basis of the relative rates of nucleation and coalescence. When the time scale of nucleation is much larger than that of coalescence, a large number of coalescence events occur between two nucleation events. Most of these will naturally contribute to growth, because the product formed can be taken up by another micelle having a nucleus before the supersaturated micelle can itself nucleate. As the coalescence time scale increases, the contribution of nucleation becomes increasingly important. By comparison of time scales at $R = 5$ and at $R = 32$, it is expected that, at $R = 32$, larger but fewer particles will be formed, whereas, at $R = 5$, larger number of particles may result. This corresponds to the experimental observations too.

On the basis of the same argument, one can explain the large differences in results seen between the two experiments with $R = 32$. A higher coalescence time scale at $x = 10$ (due to lower coalescence efficiency) encourages more nuclei, giving a much smaller value of MAN at $x = 10$, compared to that at $x = 2$.

The particle size distributions for the two experiments with $R = 32$ —i.e., with $x = 2$ and 10—obtained by simulating the reported experimental conditions⁹ are presented in Figure 9. It is seen that not only particle size but also spread are higher at $x = 2$ than for $x = 10$. The spread in the PSD is more for $x = 2$, in comparison to that for $x = 10$, as higher excess reactant in $x = 10$ results in faster reaction and hence nucleation, causing less spread in the PSD. Experimental data in Table 1 indicate that there is considerable variation in the mean value, for $R = 32, x = 2$, ranging from MAN = 35–45. Thus there exists 25% variation in the experimental mean, suggesting a possibility of high variance in the experimental PSD too. However, the experimental variance is not reported.

It is interesting that the previous simulation model³ would not be able to make any reasonable prediction of any of these data for the following reason. For example, their simulation results show that, for an excess of $x = 4$ or more, the mean particle size is almost exactly the same as the initial scaling size. For an excess of $x = 1.5$, the mean size is slightly more than 1. If one translates in terms of MAN values in the present case, the expected values from their simulation can be looked up in Table 2.

(14) Suzuki, K.; Mizutani, N.; Harada, M. *J. Chem. Eng. Jpn.* **1999**, *32*, 31.

(15) Bagwe, R. P.; Khilar, K. C. *Langmuir* **2000**, *16*, 905.

(16) Bandyopadhyaya, R.; Kumar, R.; Gandhi, K. S.; Ramkrishna, D. *Langmuir* **1997**, *13*, 3610.

(17) Weast, R. C., Ed. *Handbook of Chemistry and Physics*, 51st ed.; Chemical Rubber Co.: Cleveland, OH, 1970; p B-232.

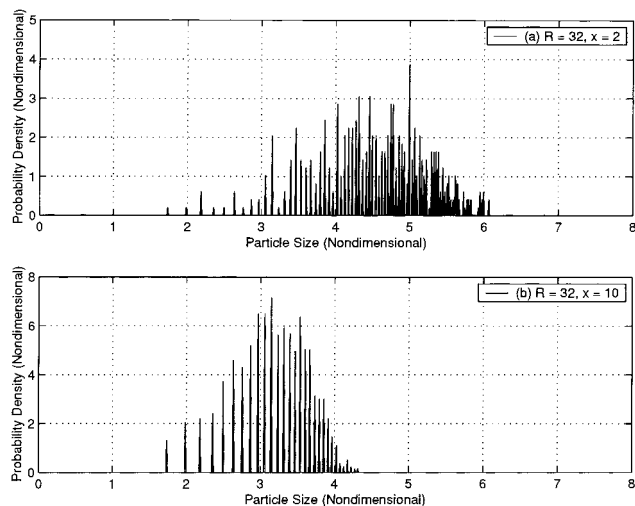


Figure 9. Comparison of PSD of CdS nanoparticles obtained from simulation for two cases: (a) $R = 32$, $x = 2$. (b) $R = 32$, $x = 10$.

Their predictions of MAN would thus correspond to near about the initial mean occupancies of the limiting reactant, Na_2S , listed in the table. On the basis of the above discussion, predictions from their simulation would be same as that of $E[\text{Na}_2\text{S}]$ for $x = 5$ and 10 and slightly more than $E[\text{Na}_2\text{S}]$ for $x = 2$. However all these values are fractional and much less than 1 and, therefore, cannot be possible on physical grounds, showing the need for a less restrictive framework like the present one.

5.3. Simulation of $\text{Fe}(\text{OH})_3$ Nanoparticle Formation. The predicted range of $\text{Fe}(\text{OH})_3$ particle size³ was lower than the experimental size range,⁴ the latter being quoted by Li and Park.³ The same experimental system was simulated by taking a total of 10^5 micelles but through the present simulation procedure. The reported $\text{Fe}(\text{NO}_3)_2$ concentration of 0.05 M in the aqueous reverse micellar core, with 30 nm size, corresponds to 425 reactant molecules in a micelle. Thus we start with 425 molecules in each micelle, there being no need of using a Poisson distribution at such a high occupancy. Half the micelles contain 425 $\text{Fe}(\text{NO}_3)_2$ molecules each, and the other half have an equal number of NH_4OH molecules.

For calculating supersaturation of $\text{Fe}(\text{OH})_3$, we used¹⁷ $K_s = 1.1 \times 10^{-36} \text{ mol}^2 \text{ L}^{-2}$ and the micellar core volume at 30 nm diameter (size reported by Pillai, 1995) was $V_{\text{mic}} = 1.41 \times 10^{-20} \text{ L}$. In the nucleation rate expression of eq 5, we used the same parametric values of $A = 278.42 \text{ s}^{-1}$ and $B = 600$, the latter due to absence of a better estimate of σ for $\text{Fe}(\text{OH})_3$. The critical number of molecules for nucleation was taken as $k_c = 5$. The parameters in eq 8 for calculating coalescence rate were maintained the same. Thus we have used $\beta_m = 0.1$ and $q_m = 1.097 \times 10^{-11} \text{ cm}^3 \text{ s}^{-1}$. Further, $N_{\text{mic}} = 10^{18} \text{ cm}^{-3}$ was used as a typical order of micellar number density (this value being not reported in the paper), valid for most reverse micellar systems.

The variation in the fractions of $\text{Fe}(\text{OH})_3(\text{l})$, $\text{Fe}(\text{OH})_3(\text{s})$, and nucleated micelles are shown in Figure 10a–c, respectively. As expected, the fraction of $\text{Fe}(\text{OH})_3(\text{l})$ in Figure 10a first grows with reaction and then falls as nucleation and growth of particles begin. On comparing Figure 10b,c, we find that nucleation stops at a point when about 90% of the initial reactant has been converted into $\text{Fe}(\text{OH})_3$ particles. The last 10% of reaction product is thus used for growth of existing particles with no further nucleation. This therefore indicates that formation of particles much smaller than the mean size—which is undesirable and occurs if nucleation continues till the

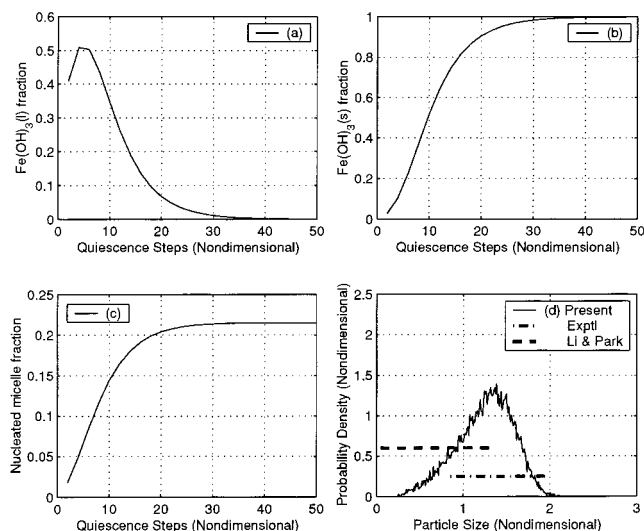


Figure 10. Temporal evolution of various quantities during simulation of $\text{Fe}(\text{OH})_3$ nanoparticles: (a) fraction of $\text{Fe}(\text{OH})_3(\text{l})$ molecules; (b) fraction of $\text{Fe}(\text{OH})_3(\text{s})$ molecules; (c) fraction of nucleated micelles; (d) comparison of experimental size range (— · —, Pillai) and simulated size range (---, Li and Park) of $\text{Fe}(\text{OH})_3$ nanoparticles with the PSD from our simulation.

end—is prevented here. The typical nucleation rate in this example corresponds to 425 molecules of $\text{Fe}(\text{OH})_3(\text{l})$, formed when two coalescing micelles contain nitrate and hydroxide, respectively. This comes out to be $k_n(425) = 7.87 \times 10^4 \text{ s}^{-1}$. The nucleation time scale is thus $1.27 \times 10^{-5} \text{ s}$, which is quite close to the coalescence time scale of $9.11 \times 10^{-7} \text{ s}$. This implies that nucleation rate is quite high and a significant fraction of micelles would form nuclei. From Figure 10c, we indeed find a high percentage of micelles (more than 22%) to form nuclei.

The final PSD shown in Figure 10d is obtained at 99.99% conversion of initial reactant to the solid phase. Of interest is the fact that the predicted PSD ranges from 0.25 to 2.05 in nondimensional scale, which on using the scaling size of 3.5 nm for this system (section 2) translates to a size range of 0.85 nm to 7.2 nm, with a mode at 4.5 nm. This corroborates much better with the experimental range of 3–7 nm (shown as a dash–dotted line), especially at the higher end of the spectrum, compared to Li and Park's predicted range of 0.2–4.7 nm (shown here as dashed line). The improved prediction from the present simulation has been possible due to inclusion of a critical nucleus size and nucleation rate in it. The former prevents nucleation below the critical. On the other hand, nucleation rate being an increasing function of supersaturation, nucleation at larger sizes is more probable in our simulation. This translates into relatively bigger particles in the PSD. Thus our predicted PSD is shifted toward higher particle sizes from that of Li and Park's, improving predictions of both the lower and the upper extremities of the particle size range. Such an effect cannot be induced in Li and Park's simulation with instantaneous nucleation rate and no critical size. Neither nucleation at small sizes can be prevented nor larger nuclei are favored, in their simulation.

6. Conclusions

The liquid–liquid mode of precipitation by mixing two sets of reverse micelles has been analyzed by Monte Carlo simulation. The previous simulation³ has severe limitations on many counts. We have developed a much more generalized framework on the basis of the concept of

interval of quiescence and by incorporating various realistic features of reaction and exchange dynamics characteristics of reverse micellar systems. The present simulation is thus able to address various relevant key issues arising in experiments. For example, the present work has successfully simulated the effects of micellar size (via change in R), reactant concentration, etc., on the mean size and size distribution of nanoparticles. This has been illustrated with the experimental data of different workers on CdS and Fe(OH)₃ nanoparticle synthesis.

The simulation algorithm is quite flexible and can be easily extended for accounting other details deemed important in explaining other experimental systems and trends than what is studied presently. It can also be utilized for making predictions of other synthesis strategies such as the fed batch mode of addition of one reactant. It is interesting to study such variants of synthesis strategies, hitherto not attempted experimentally, in exploring better ways to prepare and control particles of not only desired mean size but of specific size distribution too.

Nomenclature

A	preexponential factor of nucleation rate in micelles, s^{-1}
B	exponential term in nucleation rate expression
$[C(l)]_l$	molar concentration of a species $C(l)$ in micellar core, mol L^{-1}
$E[A]$	expected (mean) number of molecules of species A in a micelle
f_c	total fusion–fission frequency of all micelles, s^{-1}
f_n	total nucleation frequency of all micelles, s^{-1}
f_t	total frequency of all events in simulation, s^{-1}
i	index of micelle used in simulation
K_s	solubility product of a sparingly soluble salt in water, $\text{mol}^2 \text{L}^{-2}$
k_B	Boltzman's constant, $1.3806 \times 10^{-16} \text{ erg K}^{-1}$
k_c	critical number of molecules required in a micelle for nucleation
$k_n(l)$	homogeneous nucleation rate in the l th micelle in simulation, containing l molecules of $C(l)$, s^{-1}
l	number of $C(l)$ molecules in a nonnucleated micelle
M	number of quiescence steps in simulation
MAN	molecular aggregation number of CdS particle, giving number of molecules in a particle
N	total number of micelles used in simulation
N_A	Avogadro's number, $6.023 \times 10^{23} \text{ mol}^{-1}$
N_{mic}	number density of all micelles reported in experiments and used in simulation, cm^{-3}
q_m	Brownian collision frequency between micelles, $\text{cm}^3 \text{ s}^{-1}$
R	molar ratio of water to surfactant
S	solubility of a sparingly soluble salt in water, mol L^{-1}
T	temperature of experiment, K
T_Q	random variable giving quiescence time interval
t	time, s
t_Q	sample value of random quiescence interval T_Q used in simulation, s
$U[0,1)$	uniform random number generator in the half-open interval 0 to 1
u_1	a sample value of $U[0,1)$
V_m	volume of a precipitate molecule, cm^3
V_{mic}	volume of micellar core, L

x excess of a reactant used in CdS precipitation given as the ratio of the amounts of $\text{Cd}(\text{ClO}_4)_2$ to Na_2S

Greek Symbols

β_m	coalescence efficiency in intermicellar collisions
η	viscosity of continuous organic medium, $\text{g cm}^{-1} \text{ s}^{-1}$
λ_1	supersaturation in a micelle due to l molecules of any sparingly soluble salt
σ	interfacial tension between nucleus and micellar core liquid, dyn cm^{-1}
τ_s	time scale of an event involving a micelle with subscript S , s

Special Symbols

(l)	molecules in the liquid phase
(s)	molecules in the solid phase

Subscripts

c	coalescence with any micelle
n	nucleation in a single micelle

Appendix A: Binomial Redistribution of Molecules

In this appendix, we describe the binomial redistribution of molecules, during fission of the dimer into the daughter micelles. Consider two micelles, having i and j molecules of the species A , respectively, coalescing into a dimer. So there are $i + j = n_1$ molecules of A . Similarly, one can have only molecules of species B . In another scenario, consider two micelles having reactants A and B , which come together in the dimer, react, and generate n_2 molecules of the excess reactant and n_3 molecules of product $C(l)$. Hence, in general, we need to redistribute n molecules of the species A or B , and/or the species $C(l)$.

We know that Poisson distribution of solubilizate among micelles holds good when molecules migrate from one micelle to the other during collisions.¹⁸ It is further known that¹⁹ binomial redistribution of the n molecules in a dimer during its fission preserves the aforementioned Poisson distribution. So we do the following calculation in the "binomial" subroutine (see Figure 1) of our simulation code, to find out the proportion in which molecules are redistributed.

The probability that, after fission, one of the daughter micelles would get m molecules, and hence the other $n - m$ molecules, is given by the binomial probability distribution,

$$P_m = \binom{n}{m} p^m (1-p)^{n-m} \quad m = 0, 1, 2, \dots, n \quad (10)$$

Assuming the molecules do not distinguish the micelles (depending on whether it has particles or not, for example), each of the n molecules can occupy either of the daughter micelles with equal probability. Hence, $p = 1/2$. So the above equation becomes

$$P_m = \binom{n}{m} \left(\frac{1}{2}\right)^n \quad m = 0, 1, 2, \dots, n \quad (11)$$

(18) Tachiya, M. In *Kinetics of Nonhomogeneous Processes*, 1st ed.; Freeman, G. R., Ed.; John Wiley & Sons: New York, 1987; pp 575–650.

(19) Rothenberger, G.; Infelta, P. P. In *Kinetics and Catalysis in Microheterogeneous Systems*, 1st ed.; Vol. 38 of Surfactant Science Series; Gratzel, M., Kalyanasundaram, K., Eds.; Marcel Dekker: New York, 1991; pp 49–62.

Next we generate a random number from $U(0,1)$ and compare its value with the cumulative of the probability distribution given in eq 11. By the method of inversion we then get the value of m for a particular redispersion event.

Appendix B: Nondimensional Particle Size Distribution

In plotting the PSDs from our simulation, we have used nondimensional quantities. During every stage and also at the end of a simulation run, we know for each nucleated micelle how many molecules of product the particle in it has. Suppose a particle has k molecules of the precipitate product C. Then k divided by the starting (at $t = 0$) mean number of molecules of the limiting reactant, e.g. $E[A]$, gives a scaled number of molecules. This being the number of molecules is akin to the volume of the particle. So the cube root, defined as

$$S = \left(\frac{k}{E[A]} \right)^{1/3} \quad (12)$$

is akin to nondimensional particle size. This calculation is done for each particle.

Let the maximum value of S be S_{\max} . We divide the range $(0, S_{\max})$ into S_i intervals, called bins. We define $\Delta S = S_{\max}/S_i$. Typically, we have used $S_{\max} = 2$ and $S_i = 200$ bins, giving $\Delta S = 0.01$. Now for getting the nondimensional number density of particles, we do the following. First we take up each particle, and from its S value, we put it in the appropriate bin. Let N_i be the number of particles in the i th bin. Then

$$N_{\text{part}} = \frac{N_i \sum_{i=1}^{S_i} N_i}{\Delta S} \quad (13)$$

is the nondimensional number density. The PSDs shown are therefore plots of N_{part} versus S , and the total area under the plots would be 100, since $\Delta S = 0.01$.

LA000101A